LA-5789-MS
Informal Report

UC-20
Reporting Date: October 1974
Issued: November 1974

Tamped Thermonuclear Burn of DT Microspheres

by

Rodney J. Mason
Richard L. Morse

los alamos
scientific laboratory
of the University of California
LOS ALAMOS, NEW MEXICO 87544

UNITED STATES
ATOMIC ENERGY COMMISSION
CONTRACT W-7405-ENG. 36

In the interest of prompt distribution, this LAMS report was not edited by the Technical Information staff.

Printed in the United States of America. Available from
National Technical Information Service
U.S. Departmment of Commerce
5285 Port Royal Road
Springfield, VA 22151
Price: Printed Copy $4.00 Microfiche $2.25

TAMPED THERMONUCLEAR BURN OF DT MICROSPHERES

by

Rodney J. Mason and Richard L. Morse

ABSTRACT

The thermonuclear yields and gains from highly compressed DT spheres tamped by high-Z shells are calculated for temperatures near and above ignition and for tampers up to 100 times more massive than the DT. It is shown that the dynamic and structural advantages of including pusher-tamper shells need not be significantly diminished by the reduction of total fuel mass in the target.

Much discussion has been given to the laser-driven compression of homogeneous DT pellets.[1-6] Structured laser[6] and e-beam[7] fusion targets are also under consideration, in which the DT "fuel" is stored as a gas inside a thin tamper layer of metal or glass, or a shell of DT is frozen onto the inner surface of the tamper. The tamper can provide structural support--eliminating cryogenic concerns, it can ease the laser pulse shaping requirements,[8] and it may serve to shield the DT from superthermal electron preheat.[9] The use of a number of contiguous shells of various low- and high-Z materials in laser and e-beam initiated fusion targets has been under study at the Los Alamos and Livermore Laboratories for many years. The aim of the present work is to examine the effects of tamping on the efficiency of thermonuclear burn.

We assume that a laser or e-beam can be used to bring a tamped pellet core to high compressions and ignition conditions.[10] The DT will generally be hotter than the tamper, since it is compressed from a lower initial density, and since it is heated by a final strong shock,[2,6] or possibly multiple shocks[11] as the tamper inner radius closes to a minimum, while the pulse form is adjusted to minimize shock heating of the tamping material during implosion. With the increased DT opacity at high density, 3 keV is near the minimum temperature at which ignition and efficient yield production are possible in bare DT microspheres. At 10-keV, burn performance in untamped pellet cores is nearly optimal. These results were spelled out in Ref. 10. We explore this now familiar phenomenology with the addition of tamping.

Numerical Studies and Results

By computer simulation we have traced the evolution of tamped fuel configurations, such as that shown in Fig. 1. Numerous cases have been calculated with our "3T" hydro-burn code of Ref. 10. Most of the runs were for 10 μg of DT fuel m_f surrounded by from 10 μg to 1 mg of tamper material m_t: thus, the mass ratio $R_m = m_t/m_f = 1$ to 100, suitable parameters for a 10^5-J laser. The initial fuel density ranged from $\rho_f = 1.6$ to 2100 g/cm.^{3} Its electron and ion temperatures were taken as initially equal, and either at 3 or 10 keV; the radiation temperature in the DT was started at 1 keV. The tamper density was varied from 4 times the fuel density to the maximum allowed by

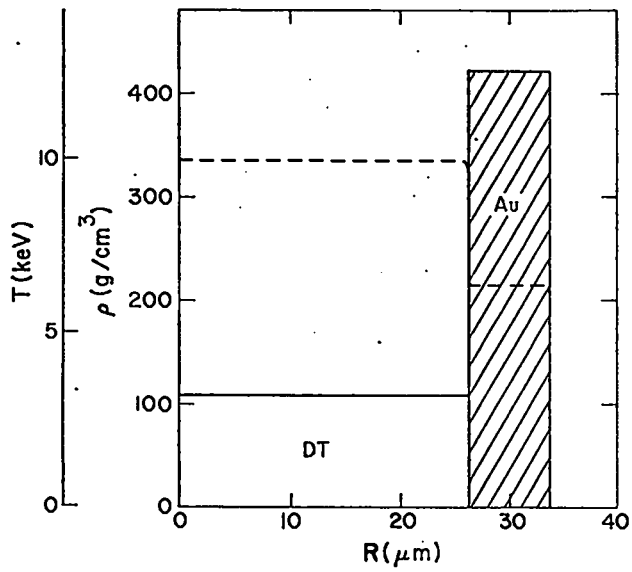

Fig. 1. Sample initial burn configuration. Fuel density ρ_f = 105 g/cm^3 _____, tamper density ρ_t = 420 g/cm^3 _____. Fuel temperature (T_i, T_e) 10 keV, gold temperature 6.4 keV - - -. m_t/m_f =10.

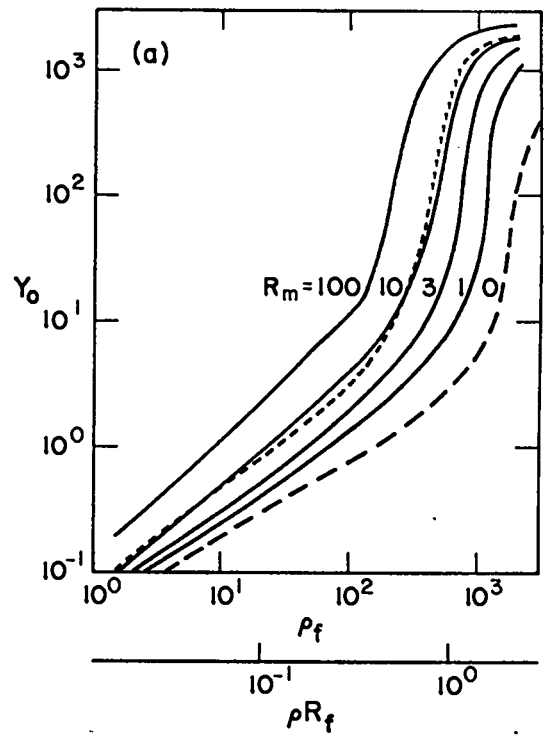

Fig. 2(a). 10 μm of DT at 3 keV, tamped with gold. The gold/DT density ratio generally 4/1; yield in kilojoules vs ρ_f (or ρR_f) for various tamper/fuel mass ratios, R_m; $\rho_t = 4\rho_f$ _____, $\rho_t = \rho_t|_{max}$ - - - -.

degeneracy. The electron, ion, and radiation temperatures in the tamper were equal and chosen to establish initial pressure equilibrium between the tamper and the fuel. This was accomplished graphically with the aid of detailed pressure plots of the Fermi-Thomas-Dirac equations of state for the DT, and for the various tamper materials. Calculations were done for tampers of gold (Z = 79, A = 179, normal density 19.3 g/cm^3), nickel (28, 58.7, 8.88 g/cm^3), and glass (10, 20, 2.2 g/cm^3).

Figure 2(a) shows the 3-keV yields Y_o obtained from 10 μg of DT for various ρ_f and R_m values and at $\rho_t/\rho_f = 4$ for the solid curves. The ρR product for the fuel $\rho R_f (\equiv \int \rho dR_f)$ is also given as a scale. The tamper is of gold. The long dashed, $R_m = 0$, untamped yield curve is from Ref. 10, Fig. 7(a). Along it, below ρR_f = 0.3 g/cm^2 we get simple $Y_o \sim \rho_f^{2/3} \sim \rho R_f$ yield scaling. Above 0.3 we observe bootstrap heating of the fuel from α-particle redeposition. (The ratio of α-particle range to the fuel radius is $0.06/\rho R_f$ at 3 keV.) Reference 10 defined the burn-up fraction to be $f_{ro} \equiv Y_o/(326 \cdot m_f)$ where Y_o is in kJ and m_f is in μg. Beyond ρR_f = 2.0 there is sufficient confinement time when $R_m = 0$ to raise the fuel temperature into the 20- to 70-keV range, where $Y_o \simeq 326 \cdot m_f \cdot \rho R_f/(6.3 + \rho R_f)$. Going to R_m = 1, and higher, we observe substantial increases in the yields, especially in the $\rho R_f > 1.0$ ignition region. Perhaps, more important, as we go from $R_m = 0$ to 100, the ignition value of ρR_f decreases from about 1.5 g/cm^3 to 0.3 g/cm^3. Addressing the tamper density dependence, we point out that the maximum tamper density is limited by degeneracy -- given the constraint of initial pressure equilibrium. At ρ_f = 2100 g/cm^3 this limit is $\rho_t/\rho_f|_{max} = 4.9$ with gold. At ρ_f = 1.6 g/cm^3 we are permitted many more multiples

of the fuel density before the gold becomes degenerate at temperatures well below the fuel value, so $\rho_t/\rho_f\big|_{max} = 217$. The short dashed, $R_m = 10$ curve shows the yield obtained at the maximum permissible gold densities. Clearly, at 3 keV the sensitivity to ρ_t is slight.

Overall burn performance is measured by the gain[10] $G_o = Y_o/(mI)$, in which mI ($m_f I_f + k_t I_t$) is the total energy invested in the fuel and tamper prior to burn. Figure 2(b) was constructed by dividing the 2(a) yields by internal energies extracted from our equation-of-state tables. The $R_m = 0$ curve goes through unity at $\rho R_f = 1.00$ and predicts a 250-fold gain at $\rho R_f = 4.4$. With tamping at low ρR_f the extra input energy demands outweigh the augmented yield from the extended confinement time. Above $\rho R_f = 0.3$, however, bootstrap heating raises the

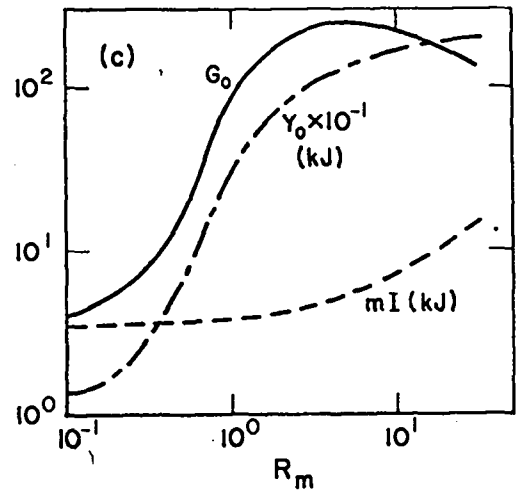

Fig. 2(c). Y_o, mI, and G_o variations with R_m for $\rho_f = 1260$ g/cm^3, $T_f = 3$ keV, and $\rho_t = 7527$ g/cm^3 = $\rho_t|_{max}$, $T_t = 250$ eV.

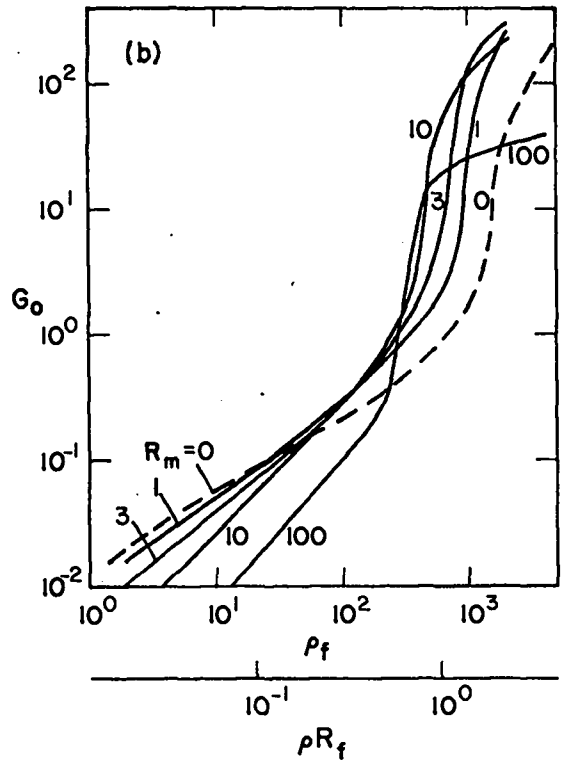

Fig. 2(b). Gain ($\equiv G_o/mI$) vs ρ_f (and ρR_f) and R_m.

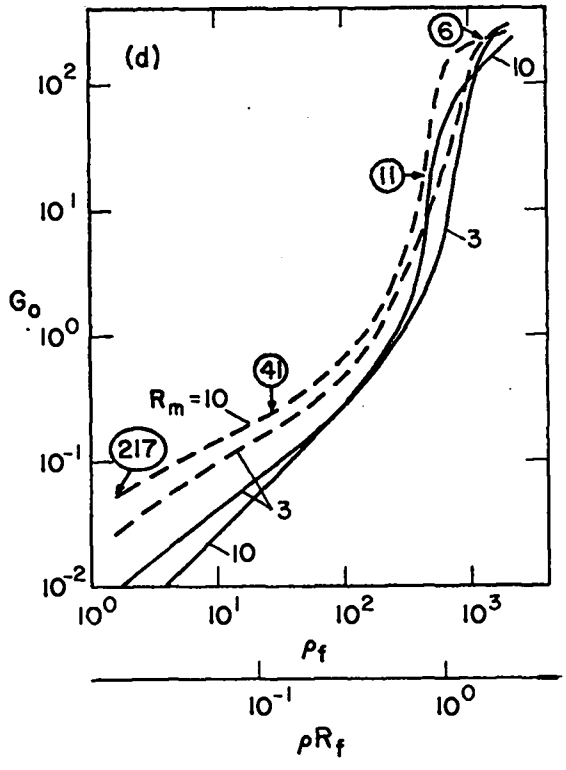

Fig. 2(d). $R_m = 3$ and 10 gains for $\rho_t/\rho_f = 4$ ____ and $\rho_t/\rho_f\big|_{max}$ ----- (maximum density ratio values circled).

DT reaction rate sufficiently so that the extra time can markedly raise the gain. At $\rho R_f = 1.4$, for example, both the $R_m = 3$ and the $R_m = 10$ tamper give a 50-fold increase in G_o. With excessive tamping, the added energy requirements again destroy G_o, as indicated by the $R_m = 100$ results. Figure 2(c) shows how, typical of the $\rho R_f > 1$ regime, the mI requirements, and yield saturation from fuel depletion [10] lead at $\rho R_f = 1.56$ ($\rho_f = 1260$ g/cm^3) to a best G_o (= 250) and an optimal R_m (=4.5). Figure 2(d) shows that the gain can improve significantly with $\rho_t \to \rho_{t|max}$, even though the yield may remain relatively constant. This is a consequence of the tamper fuel pressure equilibrium. The pressure measures energy/volume, so a denser tamper represents less deposited energy -- giving a higher G_o.

When the 3-keV yield and gain curves are plotted vs the overall confinement parameter ρR_{tot} $\left(\equiv \int \rho dR_f + \int \rho dR_t\right)$,

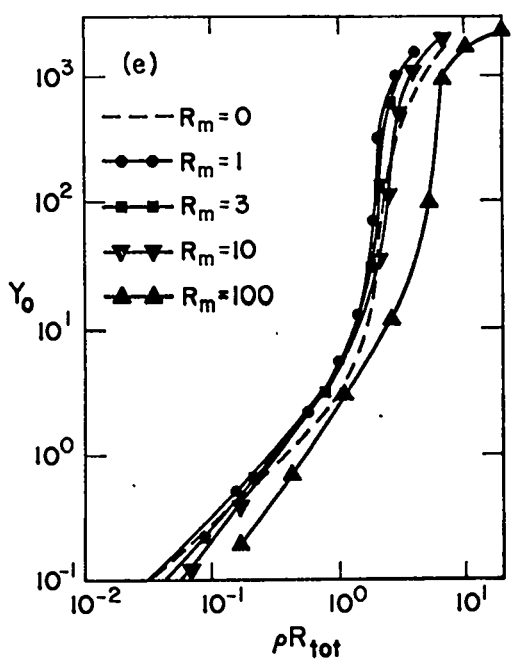

Fig. 2(e). Yield vs ρR_{tot}.

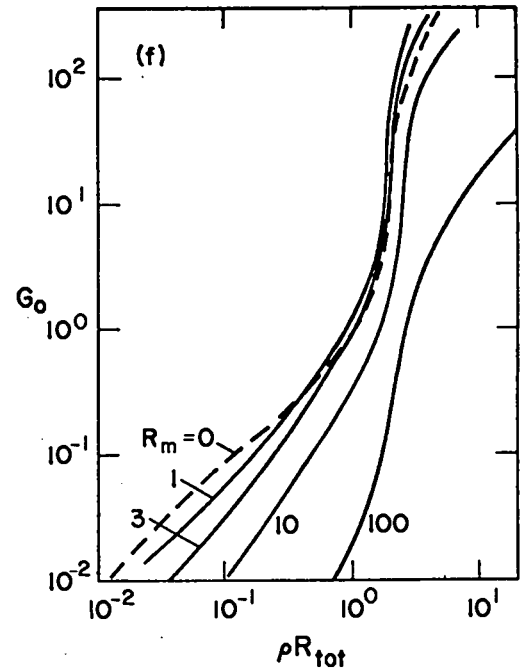

Fig. 2(f). Gain vs ρR_{tot}.

Figures 2(e) and (f), the yield curves are in close coincidence for $R_m < 10$, and even the gain curves are nearly coincident for $R_m < 3, \rho R_{tot} > 0.5$. Note that the $R_m = 1$ to 10 yields slightly exceed the untamped performance in the $0.3 < \rho R_{tot} < 2.0$ regime, since the greater tamper opacity aids the burn and ignition.

Figure 3(a) shows that our results readily scale to smaller systems when expressed in terms of burn-up fractions and ρR_{tot}. It shows good agreement as we go from 10 μg to 0.1 μg of DT at 3 keV, keeping $\rho_t/\rho_f = 4$, with a gold tamper, and $R_m = 3$. Under these conditions at $\rho R_{tot} = 1.37$, for example, there is 3.5 kJ of internal energy in the 10 μg of DT, and 2.7 kJ in the gold. Taking the efficiency of the energy transfer from the laser to the tamper-DT pellet to be 10%, this implies that 62 kJ of laser energy is deposited. Alternatively, the 0.1 μg fuelled core should require only 620 J of laser input energy.

Results for the 10-keV DT are collected in Figs. 3(b) - (d). All of the yields are,

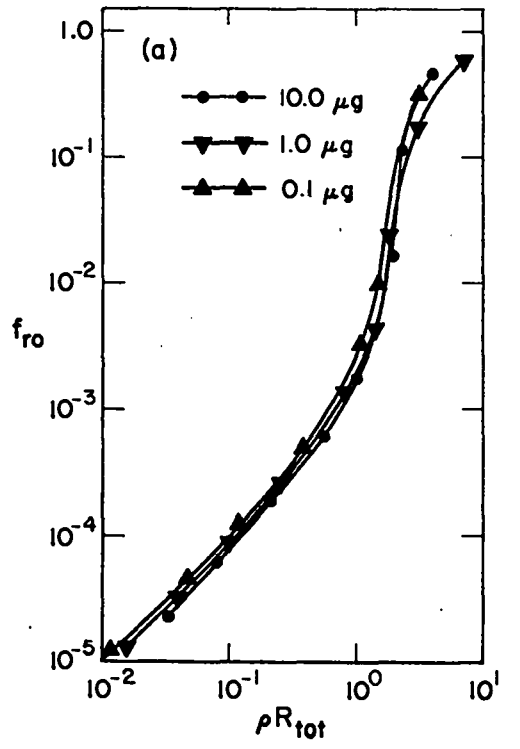

Fig. 3(a). Burn fraction f_{ro} vs ρR_{tot} from 10, 1 and 0.1 μg of DT, tamped by gold at R_m = 3 and $\rho_t/\rho_f = 4.0$.

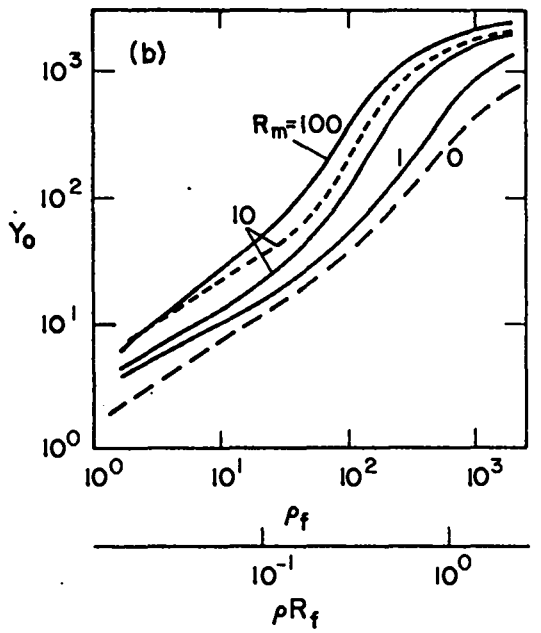

Fig. 3(b) 10 μg of DT at 10 keV and gold tampers: yield vs fuel density and R_m.

of course, higher than at 3 keV because of the $\langle\sigma v\rangle \sim T^{3.5}$ dependence of the burn rate. Here, when ρ_t goes from $4\rho_f$ to $\rho_t|_{max}$, the Y_o increase is considerable (e.g., 1.6-fold at ρ_t = 50 g/cm^3). This is because the early heat flow from the 10 keV DT to the much cooler, dense tamper (typically at only 250 eV for its pressure equilibrium in degeneracy) causes the inner surface of the tamper to explode (or, equivalently, ablate) which results in a temporary reduction of the fuel outer radius, increased confinement, and the extra yield. This explosion is too weak to be of consequence when $\rho_t/\rho_f \sim 4$, or, in general, at 3 keV. Both the 10-keV yields and gains are down for $R_m > 1$ when plotted vs ρR_{tot}, Figs. 3(c) and (d). This loss of performance does not occur at 3 keV because of the relative increase of yield from ignition is greater than at 10 keV, and tamping aids ignition. Only at $\rho_t|_{max}$ do the R_m =10 gains approach their untamped values.

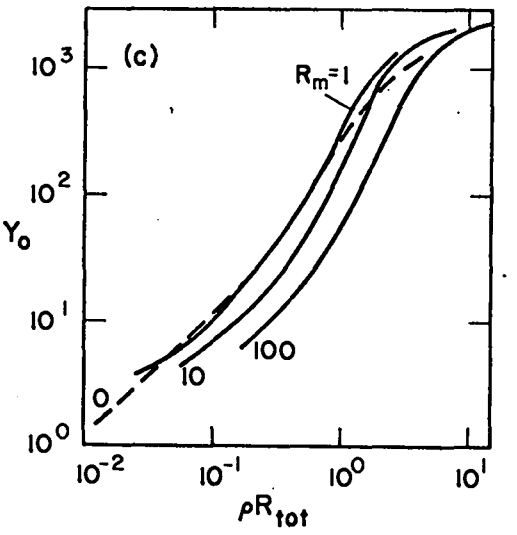

Fig. 3(c). 10 μg of DT at 10 keV and gold tampers: yield vs ρR_{tot}.

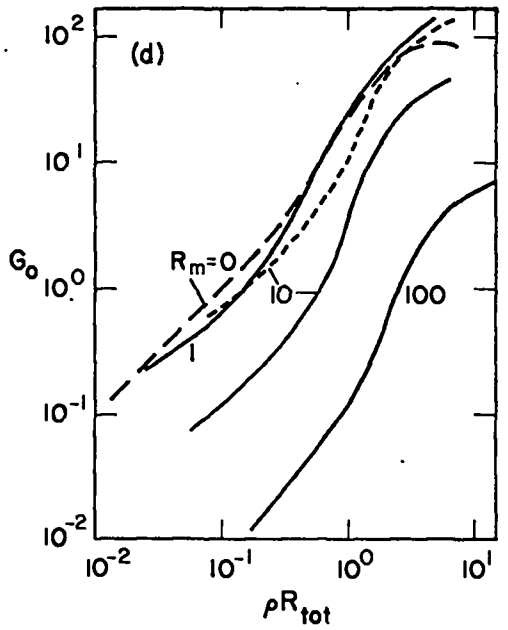

Fig. 3(d). 10 μm of DT at 10 keV and gold tampers: gain vs ρR_{tot}, showing improvements for $\rho_t \to \rho_{t|max}$ -----.

The relative insensitivity of gain to the choice of tamper materials is demonstrated by 3(e). At low ρR_{tot} the glass is

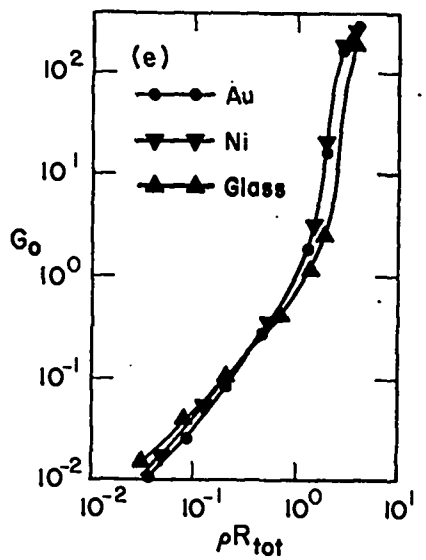

Fig. 3(e). Materials dependence: G_o vs ρR_{tot} for gold, nickel, and glass.

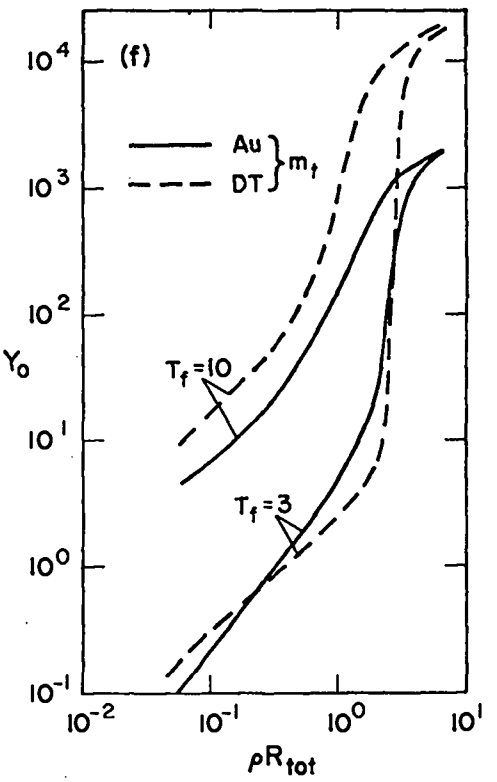

Fig. 3(f). The yield vs ρR_{tot} with first gold, then a "DT tamper" ---- at R_m = 10, ρ_t/ρ_f = 4, and T_f = 3 and 10 keV.

marginally best by requiring less internal energy to establish the pressure equilibrium. For $\rho R_{tot} > 1.0$ the situation is reversed, since the glass manifests degeneracy energy needs first.

Of course, if it were possible to replace the cold, inert tamping material with DT at the same temperature and density the results would be better in almost all cases since then the tamper itself could be ignited by propagating burn,[10] Figure 3(f) shows how the use of a "DT tamper" at R_m = 10 leads to up to 10 times the yield production obtainable with the corresponding gold tamper. An exception to this occurs at 3 keV near ρR_{tot} = 1.5, where the ρR_{tot} is too low (< 2) [10] to encourage good propagation, and the greater gold opacity encourages faster bootstrap heating.

Conclusions

A fixed amount of fuel gives an increased yield for a given ρR_f and ignites at a lower ρR_f, if tamping is added. What is more important, however, is that up to some tamper-to-fuel mass ratio (for 10 μg of DT, $R_m \gtrsim 3$ for 10 keV or $\gtrsim 10$ for 3 keV), the energy gain and fractional burn-up of a given amount of tamped fuel is very nearly a function of the total ρR of fuel and tamper, independent of R_m, provided that $\rho R_{tot} \gtrsim 1$ and $\rho R_f \gtrsim 0.3$. Since, in practice, it should be easier to obtain a given ρR_{tot} in a pellet in which the fuel is initially surrounded by a higher Z shell, we conclude that this advantage need not be diminished by reduced thermonuclear burn performance. A guideline for maximizing the gain is therefore:

1. Choose parameters which set the compressed fuel temperature at the minimum value at which ignition occurs, and, if possible, bring just the central fuel region out to $\rho R_f = 0.3$ to this temperature, with the remainder cooler to encourage propagating burn.

2. Increase the fraction of fuel mass $f_f = m_f/(m_f + m_t) = 1/(1 + R_m)$ within other constraints, until just before ρR_{tot} falls just below the ignition value, reflected in f_{ro} vs ρR_{tot}, or until 1. is violated. In addition to providing considerable fabrication convenience, the contribution of the shell can be, then, a means for manipulation of the implosion dynamics to bring ρR_{tot} to ignition values which might otherwise be inaccessible, without significantly reducing the amount of fuel that can be raised to optimized thermonuclear burn conditions.

References

1. J. Nuckolls, L. Wood, A. Thiessen and G. Zimmerman, "Laser Compression of Matter to Super-High Densities: Thermonuclear (CTR) Applications," Nature (London) 239, 139 (1972).

2. J. S. Clarke, H. N. Fisher, and R. J. Mason, "Laser-Driven Implosion of Spherical DT Targets to Thermonuclear Burn Conditions," Phys. Rev. Lett. 30, 89 (1973), and Phys. Rev. Lett. 30, 249 (1973).

3. K. Brueckner, "Laser Driven Fusion," IEEE Transactions on Plasma Sciences PS-1, 13 (1973).

4. R. Kidder, "Theory of Homogeneous Isentropic Compression and its Applications to Laser Fusion," Nucl. Fusion 14, 53 (1974).

5. K. Brueckner and S. Jorna, "Laser Driven Fusion," Rev. Mod. Phys. 46, 325 (1974).

6. R. J. Mason and R. L. Morse, "Hydrodynamics and Burn of Optimally Imploded DT Spheres," Los Alamos Scientific Laboratory report LA-5743-MS (1974) and Phys. Fluids (to be published).

7. G. Yonas, J. W. Poukey, K. R. Preswich, J. R. Freeman, A. J. Toepfer, and M. J. Clauser, "Electron Beam Focusing and Application to Pulsed Fusion," Nucl. Fusion 14, No. 5 (1974).

8. R. J. Mason, W. P. Gula, G. S. Fraley, R. C. Malone, and R. L. Morse, "Laser Driven Super Compression of Shells," Bull. Am. Phys. Soc. 19, 949 (1974).

9. K. Lee, D. B. Henderson, W. P. Gula, and R. L. Morse, "Transport of Energetic Electrons in Laser Fusion," Bull, Am. Phys. Soc. 18, 1341 (1973).

10. G. S. Fraley, E. J. Linnebur, R. J. Mason, and R. L. Morse, "Thermonuclear Burn Characteristics of Compressed Deuterium-Tritium Microspheres," Phys. Fluids 17, 474 (1974).

11. C. Evans and F. Evans, "Shock Compression of a Perfect Gas," J. Fluid Mech. 1, 399 (1956).